Metal–Oxo Photooxidants. Crystal Structure, Spectroscopy and Photophysical Properties of Neutral Luminescent *trans*-Dioxoosmium(VI) Complexes with Cyanide and Mesityl Ligands†

Kwok-Fai Chin, Yuk-Ki Cheng, Kung-Kai Cheung, Chun-Xiao Guo and Chi-Ming Che*
Department of Chemistry, The University of Hong Kong, Pokfulam Road, Hong Kong

A series of neutral osmium(VI)–oxo complexes having mesityl (mes) and cyanide ligands have been prepared and the crystal structures of $[Os^{VI}(py)_2(CN)_2(O)_2]$ (py = pyridine), $[Os^{VI}(tmen)(CN)_2(O)_2]$ (tmen = *N,N,N',N'*-tetramethylethylenediamine), $[Os^{VI}(mes)_2(phen)(O)_2]$ (phen = 1,10-phenanthroline) and $[Os^{VI}(mes)_2(tmen)(O)_2]$ determined. While $[Os(mes)_2(L–L)(O)_2]$ (L–L = chelating aromatic diimines and diamines) are non-emissive, the related $[Os(L–L)(CN)_2(O)_2]$ complexes have long-lived and emissive excited states in solution at room temperature. The $[Os(4,4'\text{-}Me_2bipy)(CN)_2(O)_2]$ (4,4'-Me_2bipy = 4,4'-dimethyl-2,2'-bipyridine) complex has a $E°(Os^{VI*}–Os^{V})$ value of 1.77 V *vs.* normal hydrogen electrode and is capable of oxidizing alkenes to the corresponding epoxides upon irradiation with UV/VIS light at room temperature.

High-valent osmium–oxo complexes usually undergo characteristic oxygen-atom transfer reactions to phosphines, sulfides and even to alkenes.[1] These reactions, however, would be enhanced upon irradiation with UV/VIS light. Previous spectroscopic studies[1b] on *trans*-dioxoosmium(VI) showed that the Os=O bonds in the $^3[(d_{xy})^1(d_{\pi^*})^1]$ ($d_{\pi^*} = d_{xz}$, d_{yz}) excited state are weaker than those in the ground state suggesting that these complexes are potential reagents for photo-induced atom-transfer reactions. In fact, they do possess interesting photochemistry, for example, *trans*-dioxoosmium(VI) complexes of macrocyclic tertiary amines have been shown to be emissive and are powerful photooxidants with $E°(Os^{VI*}–Os^{V})$ > 2.2 V *vs.* normal hydrogen electrode (NHE).[2,3] Interesting photochemistry has been found whereby *trans*-$[Os^{VI}L^1(O)_2]^{2+}$ (L^1 = 1,4,8,11-tetramethyl-1,4,8,11-tetraazacyclotetradecane) oxidizes alkenes under photolytic conditions. Studies by Creutz and co-workers[3] established further that the excited state of *trans*-$[Os^{VI}L^1(O)_2]^{2+}$ oxidizes Cl^- to Cl_2 and OH^- to $^•OH$ at rates of 4×10^5 and 1×10^7 mol dm^{-3} s^{-1} respectively. In an attempt to develop new photocatalysts *via* Scheme 1 it is essential that the dioxoosmium(VI) complexes be soluble in non-co-ordinating organic solvents. For these reasons, we set forth to study neutral *trans*-dioxoosmium(VI) complexes. Herein we describe the spectroscopic and photochemical properties of *trans*-$[Os^{VI}(L–L)(X)_2(O)_2]$ [L–L = chelating bidentate ligand; X = CN or mesityl (mes)].

Experimental

Materials.—2,2'-Bipyridine (bipy) was purchased from Aldrich. Pyridine (py) and *N,N,N',N'*-tetramethylethylenediamine (tmen) were distilled from CaH_2 before use. 4,4'-di-*tert*-Butyl-2,2'-bipyridine (4,4'-Bu^t_2bipy), 4,4'-dimethyl-2,2'-bipyridine (4,4'-Me_2bipy),[4] $[Os^{VI}(mes)_2(O)_2]$[5] and $K_2[Os^{VI}(O)_2(OH)_4]$[6] were synthesized by literature methods. Acetonitrile (Ajax AR) was distilled from $KMnO_4$, and CaH_2. Dichloromethane (Ajax AR) was purified by washing with concentrated H_2SO_4 followed by 5% aqueous Na_2CO_3 and distilled from CaH_2.

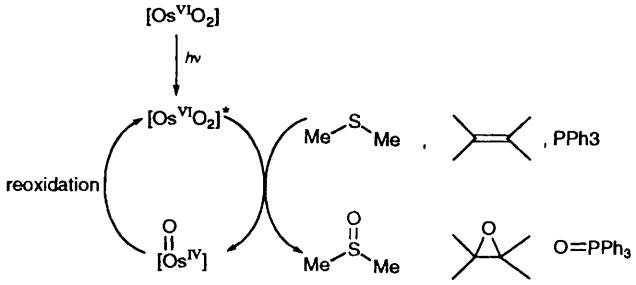

Scheme 1

Physical Measurements.—The UV/VIS absorption spectra were measured on a Perkin-Elmer Lamda 19 spectrophotometer, IR spectra as Nujol mulls on a Nicolet 20-FXC FT-IR spectrophotometer and ^{1}H NMR spectra on a JEOL model FX 270 Q spectrometer. Emission spectra were measured on a Spex Fluorolog-2 spectrofluorometer. Emission lifetime and flash-photolysis measurements were performed with a Quanta-Ray Q-switch DCR-3 Nd-YAG pulsed laser system. Sample solutions were degassed by at least four successive freeze–pump–thaw cycles. The emission quantum yields were measured by a relative method using an aqueous solution of $[Ru^{II}(bipy)_3]^{2+}$ as standard.[7] The quantum yield of the sample was determined according to equation (1), where the subscripts

$$\Phi_s = \Phi_r \left(\frac{B_r}{B_s}\right)\left(\frac{n_s}{n_r}\right)^2\left(\frac{D_s}{D_r}\right) \quad (1)$$

s and r refer to sample and reference standard solutions respectively, n is the refractive index of the solvents, D is the integrated intensity and Φ is the luminescence quantum yield. The quantity B is defined by equation (2), where A is the absorbance

$$B = (1 - 10^{-Al}) \quad (2)$$

at excitation wavelength and l is the optical pathlength.

† *Supplementary data available:* see Instructions for Authors, *J. Chem. Soc., Dalton Trans.*, 1995, Issue 1, pp. xxv–xxx.
Non-SI unit employed: eV ≈ 1.60×10^{-19} J.

Table 1 Crystallographic data for the complexes **3**, **4**, **7** and **8**

	3	**4**	**7**	**8**
Formula	$C_{12}H_{10}N_4O_2Os$	$C_8H_{16}N_4O_2Os$	$C_{24}H_{38}N_2O_2Os$	$C_{30}H_{30}N_2O_2Os$
Crystal shape	Tetragonal	Monoclinic	Trigonal	Monoclinic
M	432.44	390.44	576.78	640.79
Space group	$P4_12_12$ (no. 92)	$P2_1/n$	$P3_1$ (no. 144)	$P2_1/c$
a/Å	10.794(1)	6.190(3)	8.539(2)	9.780(2)
b/Å	10.794(1)	30.670(3)	8.539(2)	16.357(2)
c/Å	11.977(2)	6.547(1)	28.123(4)	16.898(2)
β/°	90	101.90(2)	90	105.33(1)
U/Å^3	1395.4(8)	1216.2(9)	1775.9(1.0)	2607.0(9)
Z	4	4	3	4
D_c/g cm^{-3}	2.058	2.132	1.618	1.633
μ(Mo-Kα)/cm^{-1}	91.50	104.9	54.12	49.25
F(000)	808	736	864	1264
T/K	297	297	297	297
Crystal dimensions/mm	0.10 × 0.10 × 0.15	0.1 × 0.1 × 0.3	0.10 × 0.10 × 0.15	0.15 × 0.15 × 0.35
R	0.021	0.053	0.036	0.025
R'	0.023	0.076	0.046	0.031
Scan speed/° min^{-1}	0.87–5.47	1.65–5.49	0.870–5.47	1.18–5.49

Cyclic voltammetry was performed using a Princeton Applied Research (PAR) model 175 universal programmer, model 173 potentiostat and model 179 digital coulometer. Cyclic voltammograms were recorded with a Kipp & Zonen BD90 X-Y recorder. A 0.1 mol dm^{-3} Ag–$AgNO_3$ electrode was used as the reference electrode. The working electrode was glassy carbon.

Synthesis.—$[NBu_4]_2[Os^{VI}(CN)_2(O)_2(OH)_2]$. Potassium cyanide (0.033 g) was slowly added to a solution of $K_2[Os^{VI}(O)_2(OH)_4]$ (0.093 g) in water (5 cm^3). This resulted in a change from violet to orange. The solution was stirred for 10 min. Acetic acid (0.3 mol dm^{-3}, 3.5 cm^3) was added dropwise to the solution until pH 6 was reached. Addition of NBu_4Br gave $[NBu_4]_2[Os^{VI}(CN)_2(O)_2(OH)_2]$ as a yellow-orange solid. This was recrystallized by diffusion of diethyl ether into acetone (Found: C, 39.55; H, 6.85; N, 7.80. Calc. for $C_{36}H_{74}N_6O_6Os_2$: C, 40.50; H, 7.00; N, 7.85%). IR: ν_{asym}(Os=O) 832 cm^{-1}.

$[Os^{VI}(L–L)(CN)_2(O)_2]$ [L–L = 4,4′-Me_2bipy **1**, 4,4′-Bu^t_2bipy **2**, 2 (py)$_2$ **3** *or* tmen **4**]. A slight excess of ligand was added to a dichloromethane solution of $[NBu_4]_2[Os^{IV}(CN)_2(O)_2(OH)_2]$ containing 1 drop of glacial acetic acid. After heating the solution at 40 °C for 20 min, a yellow-orange solid formed (yield 80%). The solid was washed with cold dichloromethane and stored under nitrogen. Complex **1** (Found: C, 35.85; H, 2.15; N, 11.70. Calc. for $C_{14}H_{12}N_4O_2Os$: C, 36.70; H, 2.65; N, 12.20%); IR (KBr pellet): ν_{asym}(Os=O) 846 cm^{-1}; ^{1}H NMR (CD_3CN): δ 9.53 (d, 2 H), 8.53 (s, 2 H), 7.81 (d, 2 H), 2.68 (s, 6 H). Complex **2** (Found: C, 43.90; H, 4.05; N, 10.10. Calc. for $C_{20}H_{24}N_4O_2Os$: C, 44.25; H, 4.45; N, 10.30%); IR (KBr pellet): ν_{asym}(Os=O) 851 cm^{-1}; ^{1}H NMR (CD_3CN): δ 9.60 (d, 2 H), 8.65 (s, 2 H), 8.00 (dd, 2 H), 1.51 (s, 18 H). Complex **3** (Found: C, 32.60; H, 2.15; N, 11.70. Calc. for $C_{12}H_{10}N_4O_2Os$: C, 33.35; H, 2.35; N, 12.95%); IR (KBr pellet); ν_{asym}(Os=O) 854 cm^{-1}; ^{1}H NMR (CD_3CN): δ 8.79 (d, 4 H), 8.22 (t, 2 H), 7.74 (t, 4 H). Complex **4** (Found: C, 23.75; H, 3.90; N, 13.60. Calc. for $C_8H_{16}N_4O_2Os$: C, 24.60; H, 4.15; N, 14.35%); IR (KBr pellet): 855 cm^{-1}; ^{1}H NMR (CD_3CN): 3.26 (s, 4 H), 3.10 (s, 12 H).

$[Os^{VI}(L–L)Cl_2(O)_2]$ (L = bipy **5** *or* 4,4′-Bu^t_2bipy **6**). The salt $K_2[Os^{VI}(O)_2(OH)_4]$ was dissolved in MeOH (10 cm^3) forming a clear blue solution. A slight excess of the appropriate bipyridine was slowly added. The mixture was stirred for 30 min. A few drops of concentrated HCl were added resulting in the precipitation of an orange solid. The solid was filtered off and washed with diethyl ether. Complex **5** (Found: C, 21.20; H, 1.15; N, 5.00. Calc. for $C_{10}H_8Cl_2N_2O_2Os$. C, 22.75; H, 1.25; N, 5.30%); IR (KBr pellet): ν_{asym}(Os=O) 857 cm^{-1}. Complex **6** (Found: C, 37.90; H, 4.50; N, 4.65. Calc. for $C_{18}H_{24}Cl_2N_2O_2Os$: C, 38.50; H, 4.30; N, 5.00%); IR (KBr pellet): ν_{asym}(Os=O) 846 cm^{-1}.

$[Os^{VI}(mes)_2(L–L)(O)_2]$ [L = tmen **7** *or* phen **8** (phen = 1,10-phenanthroline)]. The chelating ligand, tmen or phen (0.22 mmol), was added to an ethereal solution (20 cm^3) of $[Os(mes)_2(O)_2]$ (0.22 mmol). An orange precipitate formed immediately. The mixture was then stirred for 2 h. Solvent was removed under vacuum and the residue was extracted with diethyl ether. Crystals were obtained by concentrating the solution and cooling at −20 °C. Complex **7** (Found: C, 50.00; H, 6.15; N, 4.85; Calc. for $C_{24}H_{38}N_2O_2Os$; C, 50.00; H, 6.65; N, 4.85%); IR: ν_{asym}(Os=O) 878 cm^{-1}; ^{1}H NMR ($CDCl_3$): δ 7.26 (s, 4 H), 2.59 (s, 4 H), 2.47 (s, 6 H), 2.43 (s, 12 H), 2.30 (s, 12 H). Complex **8** (Found: C, 56.60; H, 4.40; N, 4.85; Calc. for $C_{30}H_{30}N_2O_2Os$: C, 56.25; H, 4.70; N, 4.35%); IR (KBr pellet): ν_{asym}(Os=O) 870 cm^{-1}; ^{1}H NMR ($CDCl_3$): δ 9.24 (dd, 2 H), 8.54 (dd, 2 H), 8.03 (s, 2 H), 7.86 (dd, 2 H), 7.12 (s, 4 H), 2.49 (s, 12 H), 2.46 (s, 6 H).

X-Ray Crystallography.—The crystal data for the complexes **3**, **4**, **7** and **8** are summarized in Table 1. X-Ray diffraction data were collected on an Enraf-Nonius CAD-4 diffractometer with graphite-monochromated Mo-Kα radiation (λ = 0.710 73 Å) using ω–2θ scan mode at 297 K. Intensity data were corrected for Lorentz and polarization effects and empirical absorption based on the ψ scan of five strong reflections. The structures were solved by the Patterson and Fourier methods and subsequent refinement by full-matrix least squares using the Enraf-Nonius SDP-1985 programs[8] on a Micro VAX II computer. The non-hydrogen atoms were refined anisotropically and H atoms at calculated positions with thermal parameters equal to 1.3 times that of the attached C atoms were not refined. 2348, 3240, 3562 and 1776 independent reflections having $F_o \geqslant 3\sigma(F_o)$ were used in the structure refinement of complexes **3**, **4**, **7** and **8** respectively. Convergence for 87, 136, 316 and 261 variable parameters by least-squares refinement on F with $w = 4F_o^2/\sigma^2(F_o^2)$ was reached at R = 0.021, 0.053, 0.025 and 0.036, R' = 0.023, 0.076, 0.031 and 0.046 with goodness of fit of 0.88, 2.49, 1.28 and 1.15 for **3**, **4**, **7** and **8** respectively. Final Fourier-difference maps were featureless, with maximum positive and negative peaks of 0.86 and 1.45 (**3**), 0.72 and 1.06 (**4**), 0.76 and 1.20 (**7**) and 0.54 and 0.83 e Å^{-3} (**8**). Table 2 lists the atomic coordinates for the non-hydrogen atoms and Table 3 selected bond distances and angles.

Additional material available from the Cambridge Crystallographic Data Centre comprises H-atom coordinates, thermal parameters and remaining bond lengths and angles.

Table 2 Atomic coordinates for complexes **3**, **4**, **7** and **8** with estimated standard deviations in parentheses

Atom	*x*	*y*	*z*	Atom	*x*	*y*	*z*
Complex **3**							
Os	0.081 88(4)	0.082	0.000	C(2)	−0.197 4(5)	0.135 6(5)	−0.020 4(6)
O(1)	0.111 6(3)	0.036 9(4)	0.136 8(3)	C(3)	−0.323 8(6)	0.127 0(6)	−0.000 5(6)
N(1)	0.367 6(5)	0.095 5(5)	−0.061 9(5)	C(4)	−0.363 5(6)	0.053 2(6)	0.086 9(6)
N(2)	−0.114 4(4)	0.071 8(4)	0.040 3(4)	C(5)	−0.278 9(6)	−0.012 1(8)	0.148 7(5)
C(1)	0.265 8(6)	0.089 0(5)	−0.038 4(4)	C(6)	−0.155 6(6)	−0.000 1(7)	0.122 4(4)
Complex **4**							
Os	0.195 37(9)	0.121 57(2)	0.019 6(1)	C(2)	0.562(3)	0.112 3(6)	0.394(3)
O(1)	−0.007(2)	0.127 3(4)	0.164(2)	C(3)	0.210(3)	0.212 4(6)	0.233(3)
O(2)	0.419(2)	0.116 7(4)	−0.105(2)	C(4)	0.548(3)	0.195 8(6)	0.118(4)
N(1)	0.367(2)	0.175 7(4)	0.205(2)	C(5)	0.252(3)	0.062 8(6)	0.414(3)
N(2)	0.388(2)	0.082 6(4)	0.279(2)	C(6)	0.509(4)	0.044 9(6)	0.203(4)
N(3)	−0.037(3)	0.186 9(5)	−0.335(3)	C(7)	0.036(2)	0.161 7(6)	−0.213(3)
N(4)	−0.060(4)	0.040 1(6)	−0.221(3)	C(8)	0.034(3)	0.069 2(6)	−0.135(3)
C(1)	0.458(3)	0.156 4(6)	0.418(3)				
Complex **7**							
Os	0.094 31(6)	0.094 37(6)	0.000	C(11)	0.551(2)	0.319(2)	0.100 8(7)
O(1)	0.169(1)	−0.056(1)	−0.006 6(4)	C(12)	0.501(2)	0.387(2)	0.138 2(5)
O(2)	−0.056(1)	0.172(1)	0.009 5(4)	C(13)	0.344(2)	0.393(2)	0.133 2(5)
N(1)	−0.108(1)	−0.141(2)	0.052 7(5)	C(14)	0.232(2)	0.322(2)	0.095 4(7)
N(2)	−0.145(2)	−0.105(2)	−0.052 6(5)	C(15)	0.065(2)	0.355(2)	0.097 4(7)
C(1)	−0.220(3)	−0.287(3)	0.025 3(8)	C(16)	0.624(2)	0.463(2)	0.182 5(6)
C(2)	−0.288(2)	−0.226(2)	−0.018 6(8)	C(17)	0.528(2)	0.196(2)	0.022 4(6)
C(3)	0.246(2)	0.277(2)	−0.055 7(5)	C(18)	0.347(2)	0.063(2)	−0.093 3(7)
C(4)	0.251(2)	0.447(2)	−0.057 9(5)	C(19)	0.471(3)	0.624(2)	−0.180 0(7)
C(5)	0.321(2)	0.551(2)	−0.099 2(6)	C(20)	0.194(2)	0.526(2)	−0.017 2(7)
C(6)	0.390(2)	0.505(2)	−0.137 0(5)	C(21)	−0.007(3)	−0.208(2)	0.083 3(8)
C(7)	0.389(2)	0.341(2)	−0.132 6(6)	C(22)	−0.214(3)	−0.101(3)	0.088 3(7)
C(8)	0.324(2)	0.229(2)	−0.092 9(5)	C(23)	−0.205(3)	0.002(3)	−0.081 0(7)
C(9)	0.278(2)	0.248(2)	0.056 5(6)	C(24)	−0.098(3)	−0.211(2)	−0.084 4(8)
C(10)	0.445(2)	0.248(1)	0.059 8(5)				
Complex **8**							
Os	−0.162 40(2)	0.148 23(1)	0.156 15(1)	C(14)	−0.392 6(7)	0.036 17(4)	0.214 6(4)
O(1)	−0.035 2(4)	0.177 8(3)	0.107 3(2)	C(15)	−0.325 9(6)	0.285 6(4)	0.217 5(3)
O(2)	−0.299 6(4)	0.097 1(2)	0.181 6(2)	C(16)	−0.164 3(7)	0.317 1(5)	0.034 1(4)
N(1)	−0.090 5(5)	0.021 8(3)	0.123 6(3)	C(17)	−0.447 8(9)	0.505 1(5)	0.160 3(5)
N(2)	−0.306 1(4)	0.115 3(3)	0.028 9(3)	C(18)	−0.341 0(7)	0.229 0(4)	0.285 8(4)
C(1)	−0.025 4(6)	0.152 8(3)	0.275 8(3)	C(19)	0.024 2(6)	−0.019 2(4)	0.164 2(4)
C(2)	−0.027 3(6)	0.091 5(4)	0.334 3(3)	C(20)	0.063 8(6)	−0.093 5(4)	0.136 4(4)
C(3)	0.070 7(6)	0.090 5(4)	0.410 1(4)	C(21)	−0.016 4(6)	−0.126 9(4)	0.066 8(4)
C(4)	0.175 2(7)	0.147 1(4)	0.432 6(4)	C(22)	−0.136 9(6)	−0.085 4(3)	0.020 9(3)
C(5)	0.180 8(7)	0.206 9(4)	0.376 0(5)	C(23)	−0.167 0(5)	−0.009 1(3)	0.050 9(3)
C(6)	0.083 4(6)	0.212 2(4)	0.298 1(4)	C(24)	−0.285 5(5)	0.038 2(3)	0.003 4(3)
C(7)	−0.136 0(7)	0.021 6(4)	0.321 9(4)	C(25)	−0.229 5(6)	−0.117 1(4)	−0.053 2(4)
C(8)	0.282 4(9)	0.145 3(5)	0.516 3(5)	C(26)	−0.344 6(6)	−0.076 3(4)	−0.094 0(4)
C(9)	0.104 2(7)	0.281 3(4)	0.243 0(4)	C(27)	−0.375 5(5)	0.003 5(3)	−0.067 9(4)
C(10)	−0.247 6(6)	0.265 5(3)	0.160 7(3)	C(28)	−0.493 4(5)	0.049 7(4)	−0.109 7(3)
C(11)	−0.241 7(6)	0.326 4(4)	0.102 0(4)	C(29)	−0.514 5(6)	0.125 5(4)	−0.082 2(4)
C(12)	−0.303 7(6)	0.402 2(4)	0.103 9(4)	C(30)	−0.418 3(6)	0.156 0(3)	−0.013 6(4)
C(13)	−0.380 1(6)	0.422 1(4)	0.159 4(4)				

Molecular Orbital Calculations.—Extended-Hückel molecular-orbital (EHMO) calculations were carried out on complexes **4** and **7** using the ICON program.[9] The geometric factors were obtained fron X-ray diffraction data. After transformation of the Cartesian coordinates, the Os atom was designated at the origin with N(1), Os and C(8) lying on the *x* axis and N(2), Os and C(7) lying on the *y* axis while O(1), Os and O(2) are located on the *z* axis in complex **4**. A total of 31 atoms and 81 valence orbitals, in which 44 are occupied, were employed. In complex **7** N(1), Os and C(3) lie on the *x* axis and N(2), Os and C(9) lie on the *y* axis while O(1), Os and O(2) are located on the *z* axis. A total of 67 atoms and 159 valence orbitals, in which 82 are occupied, were employed. The Os parameters were taken from Jorgensen and Hoffmann[10] whilst the others acquired are standard values.[11]

Photochemical Oxidation of Alkenes.—Photooxidation was performed by dissolving complex **1** (30 mg) in degassed acetonitrile (40 cm^3) in quartz tubes containing the organic substrates, followed by degassing with argon for 20 min. The photochemical reactions usually took 4–5 h for completion. Control experiments in the absence of **1** were performed for each reaction. Gas chromatographic analyses were conducted using a Hewlett-Packard 5890 series II chromatograph with a flame ionization detector, HP-17 column (cross-linked 50% methyl phenyl silicone, film thickness 0.2μm) and high-purity nitrogen as the carrier gas. Components were identified by comparing retention times with those of authentic samples as well as by gas chromatographic–mass spectral analysis. Quantification of individual gas chromatographic components was by the internal standard method employing a Hewlett-Packard 3396 series II electronic integrator.

Table 3 Selected bond distances (Å) and angles (°) for complexes **3**, **4**, **7** and **8**

Complex **3**			
Os–O(1)	1.739(4)	Os–C(1)	2.039(6)
Os–N(2)	2.175(4)		
O(1)–Os–O(1′)	172.3(2)	O(1)–Os–N(2)	87.6(2)
N(2)–Os–N(2′)	87.3(2)	O(1)–Os–C(1)	92.6(2)
C(1)–Os–C(1′)	88.7(3)	N(2)–Os–C(1)	179.3(2)
Complex **4**			
Os–O(1)	1.73(1)	Os–N(2)	2.21(1)
Os–O(2)	1.75(1)	Os–C(7)	2.04(2)
Os–N(1)	2.20(1)	Os–C(8)	2.05(2)
O(1)–Os–O(2)	174.6(5)	O(2)–Os–C(8)	93.1(7)
O(1)–Os–N(1)	86.8(5)	N(1)–Os–N(2)	82.0(5)
O(1)–Os–N(2)	88.4(6)	N(1)–Os–C(7)	93.5(6)
O(1)–Os–C(7)	93.1(6)	N(1)–Os–C(8)	176.2(7)
O(1)–Os–C(8)	90.9(7)	N(2)–Os–C(7)	175.2(6)
O(2)–Os–N(1)	89.0(6)	N(2)–Os–C(8)	95.0(6)
O(2)–Os–N(2)	87.5(6)	C(7)–Os–C(8)	89.6(7)
O(2)–Os–C(7)	90.7(6)		
Complex **7**			
Os–O(1)	1.734(4)	Os–N(2)	2.301(4)
Os–O(2)	1.730(4)	Os–C(1)	2.110(5)
Os–N(1)	2.298(5)	Os–C(10)	2.102(6)
O(1)–Os–O(2)	162.7(2)	O(2)–Os–C(10)	95.2(3)
O(1)–Os–N(1)	80.5(2)	N(1)–Os–N(2)	73.4(1)
O(1)–Os–N(2)	87.6(2)	N(1)–Os–C(1)	96.0(2)
O(1)–Os–C(1)	95.3(2)	N(1)–Os–C(10)	168.6(2)
O(1)–Os–C(10)	96.0(2)	N(2)–Os–C(1)	168.4(2)
O(2)–Os–N(1)	86.1(2)	N(2)–Os–C(9)	170.5(4)
O(2)–Os–N(2)	78.4(2)	C(1)–Os–C(10)	95.6(2)
O(2)–Os–C(1)	96.7(2)		
Complex **8**			
Os–O(1)	1.70(1)	Os–N(2)	2.41(1)
Os–O(2)	1.73(1)	Os–C(3)	2.13(1)
Os–N(1)	2.41(1)	Os–C(9)	2.16(1)
O(1)–Os–O(2)	158.5(3)	O(2)–Os–C(9)	96.1(5)
O(1)–Os–N(1)	79.6(5)	N(1)–Os–N(2)	77.5(5)
O(1)–Os–N(2)	84.4(5)	N(1)–Os–C(3)	170.8(4)
O(1)–Os–C(3)	98.7(6)	N(1)–Os–C(9)	93.1(4)
O(1)–Os–C(9)	96.1(6)	N(2)–Os–C(3)	93.4(4)
O(2)–Os–N(1)	82.1(5)	N(2)–Os–C(9)	170.5(4)
O(2)–Os–N(2)	80.6(5)	C(3)–Os–C(9)	96.1(5)
O(2)–Os–C(3)	97.6(6)		

Results and Discussion

The synthesis of the $[Os^{VI}(mes)_2(L–L)(O)_2]$ complexes followed the procedure developed by Wilkinson and co-workers.[5] Essentially, they are prepared by treating the co-ordinatively unsaturated $[Os^{VI}(mes)_2(O)_2]$ with the appropriate chelating ligand. The $[Os^{VI}(L–L)(CN)_2(O)_2]$ complexes are prepared from $[NBu_4]_2[Os^{VI}(CN)_2(O)_2(OH)_2]$.[12] In the presence of glacial acetic acid, the two co-ordinated OH^- groups of $[Os^{VI}(CN)_2(O)_2(OH)_2]^{2-}$ are easily substituted by the appropriate ligands. The reactions of $K_2[Os^{VI}(O)_2(OH)_4]$ with L–L in methanol followed by treatment with concentrated HCl gave the desired $[Os^{VI}(L–L)Cl_2(O)_2]$ in high yield. All the newly prepared dioxoosmium(VI) complexes are stable in the solid state. However, **3** and **4** are not very stable at room temperature and have to be stored in the dark and refrigerated. Their IR spectra show an intense $\nu_{asym}(OsO_2)$ stretch at 832–878 cm^{-1}.

The UV/VIS spectral data are listed in Table 4. For $[Os^{VI}(L–L)(CN)_2(O)_2]$, there are two vibronic structured absorption bands, I at 311–322 and II at 365–371 nm. There are also weak absorptions tailing from 400 to 600 nm. Fig. 1 shows the UV/VIS absorption spectrum of complex **4**. Previously, we assigned the vibronic structured absorption bands of *trans*-$[Os^{VI}L^1(O)_2]^{2+}$ at 300–320 and 345–370 nm to the spin-allowed and spin-forbidden $(d_{xy})^2 \longrightarrow (d_{xy})^1(d_{\pi^*})^1$ transition respectively.[2,13] However, Sartori and Preetz[12] assigned the similar absorption bands of $[NBu_4]_2[Os^{VI}(CN)_2(O)_2(OH)_2]$ to the spin-allowed singlet-singlet and singlet-triplet $p_\pi(O^{2-}) \longrightarrow d_{\pi^*}(Os^{VI})$ ($d_{\pi^*} = d_{xz}$, d_{yz}) transitions respectively. A detailed spectroscopic study recently undertaken by Gray and co-workers[14] on *trans*-dioxoosmium(VI) and *trans*-dioxorhenium(V) led to similar assignments. Thus, our previous assignment of d^2 *trans*-dioxo metal complexes needs revision. We assign band I and band II to the spin-allowed and spin-forbidden $p_\pi(O^{2-}) \longrightarrow d_{\pi^*}(Os^{VI})$ ligand-to-metal charge transfer (l.m.c.t.) transitions respectively. The $(d_{xy}) \longrightarrow (d_{\pi^*})$ transition would occur at ≈400–500 nm. In fact, the excitation spectrum of the emission of complex **4** recorded in butyronitrile glass at 77 K (Fig. 2) shows a vibronic structured absorption band at 400–500 nm, which could be assigned to $(d_{xy})^2 \longrightarrow (d_{xy})^1(d_{\pi^*})^1$. The insensitivity of λ_{max} to the variation in L–L is not unexpected, since the $p_\pi(O^{2-}) \longrightarrow d_{\pi^*}(Os)$ transition does not involve the d_{σ^*} orbital. For complexes **1** and **2** the higher energy bands are not resolved and their ε_{max} values are approximately ten times higher than those of **3** and **4**. Since

Table 4 UV/VIS spectral data for $[Os^{VI}(L–L)(CN)_2(O)_2]$ and $[Os^{VI}(L–L)Cl_2(O)_2]$ in solution at 298 ± 2 K

Complex	λ_{max}/nm (ε_{max}/$dm^3\ mol^{-1}\ cm^{-1}$)
1 $[Os^{VI}(4,4'\text{-}Me_2bipy)(CN)_2(O)_2]^a$	371 (sh) (2.0 × 10^2)
	311 (1.1 × 10^4)
2 $[Os^{VI}(4,4'\text{-}Bu^t_2bipy)(CN)_2(O)_2]^a$	371 (sh) (1.8 × 10^2)
	313 (9.6 × 10^3)
3 $[Os^{VI}(py)_2(CN)_2(O)_2]^a$	367 (2.2 × 10^2)
	318 (1.1 × 10^3)
4 $[Os^{VI}(tmen)(CN)_2(O)_2]^a$	365 (2.1 × 10^2)
	322 (8.1 × 10^2)
5 $[Os^{VI}(bipy)Cl_2(O)_2]^b$	317 (1.2 × 10^4)
	309 (sh) (1.1 × 10^4)
6 $[Os^{VI}(4,4'\text{-}Bu^t_2bipy)Cl_2(O)_2]^b$	315 (1.1 × 10^4)
$[NBu_4]_2[Os^{VI}(CN)_2(O)_2(OH)_2]^a$	368 (4.8 × 10^2)
	319 (2.0 × 10^3)
7 $[Os^{VI}(mes)_2(tmen)(O)_2]^b$	696 (3.3 × 10^2)
	410 (3.0 × 10^3)
	323 (sh) (3.3 × 10^3)
	283 (9.2 × 10^3)
8 $[Os^{VI}(mes)_2(phen)(O)_2]^b$	458 (1.2 × 10^3)
	345 (3.0 × 10^3)
	326 (4.1 × 10^3)
	267 (6.2 × 10^4)

[a] In MeCN. [b] In CH_2Cl_2.

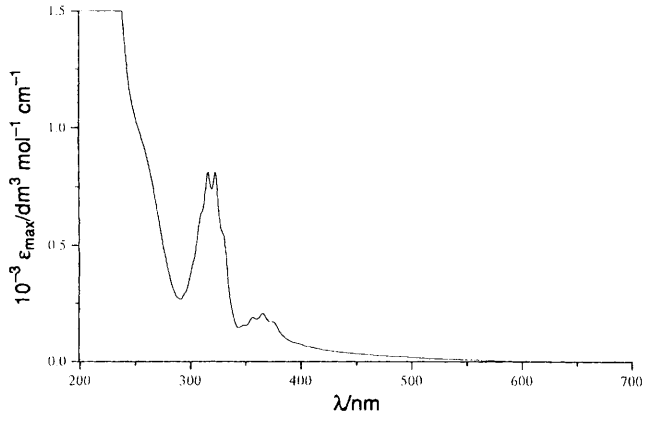

Fig. 1 UV/VIS absorption spectrum of $[Os^{VI}(tmen)(CN)_2(O)_2]$ **4** in acetonitrile

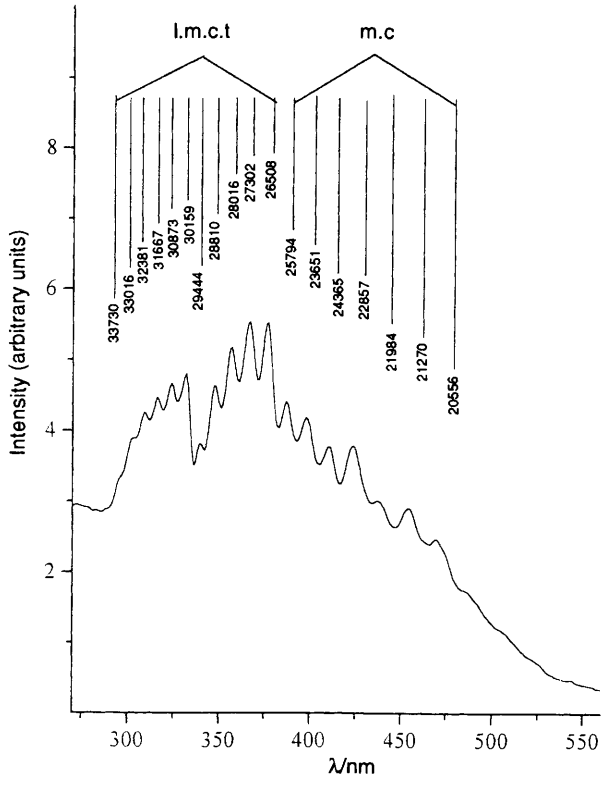

Fig. 2 Excitation spectrum of the emission of $[Os^{VI}(tmen)(CN)_2(O)_2]$ **4** in butyronitrile glass at 77 K

the free ligands (4,4′-Me_2bipy and 4,4′-Bu^t_2bipy) also have absorption bands at similar energies, these high energy bands may comprise of both the l.m.c.t. transition and the $\pi \longrightarrow \pi^*$ transition of the substituted bipy ligand. The UV/VIS spectral data of $[Os^{VI}(L\text{–}L)Cl_2(O)_2]$ are very similar to those of complexes **1** and **2**. In the absence of added L the UV/VIS absorption spectra of $[Os^{VI}(mes)_2(L\text{–}L)(O)_2]$ show absorption bands at 696 and 410 nm, presumably these come from $[Os^{VI}(mes)_2(O)_2]$ *via* reaction (3). As expected, the reaction is

$$[Os^{VI}(mes)_2(L\text{–}L)(O)_2] \xrightarrow[CH_2Cl_2]{} [Os^{VI}(mes)_2(O)_2] + L\text{–}L \quad (3)$$

suppressed by the addition of L–L. Fig. 3 shows the UV/VIS spectrum of complex **7** ($\approx 10^{-4}$ mol dm^{-3}) in the presence of 0.5 cm^3 tmen. The absorption bands at 696 and 410 nm are absent, however, the absorption at 322 nm is considerably more intense than that in $[Os^{VI}(L\text{–}L)(CN)_2(O)_2]$.

Crystal and Electronic Structures.—Perspective views showing the molecular structure of complexes **3**, **4**, **7** and **8** are given in Figs. 4, 5, 6 and 7 respectively. These four complexes adopt a distorted octahedral co-ordination geometry with a bent O=Os=O angle. The measured Os=O distances [1.70(1)–1.739(5) Å], are comparable to those values found in most *trans*-dioxoosmium(VI) complexes. In complex **3**, the two co-ordinated pyridine ligands are aligned along the O=Os=O parallel plane, presumably this is owing to steric factors. For similar reasons, the two mesityl groups in **7** are almost at right angles to the plane defined by atoms N(1), N(2), C(3) and C(9). Similar geometry of the two mesityl ligands is found in complex **8**.

An intriguing structural feature of complexes **7** and **8** is the short intramolecular distance between the Os=O unit and one of the H atoms of the mesityl ligands. For **7**, the H(18)–O(1) and H(15)–O(2) distances are calculated to be 1.91 and 1.96 Å

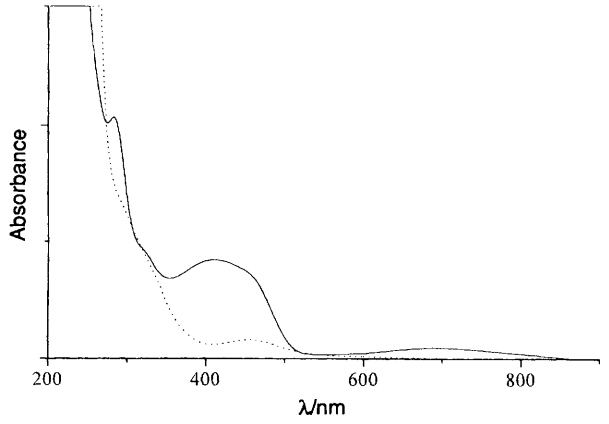

Fig. 3 UV/VIS absorption spectrum of $[Os^{VI}(mes)_2(tmen)(O)_2]$ **7** in the presence (· · · ·) and absence (——) of tmen in acetonitrile

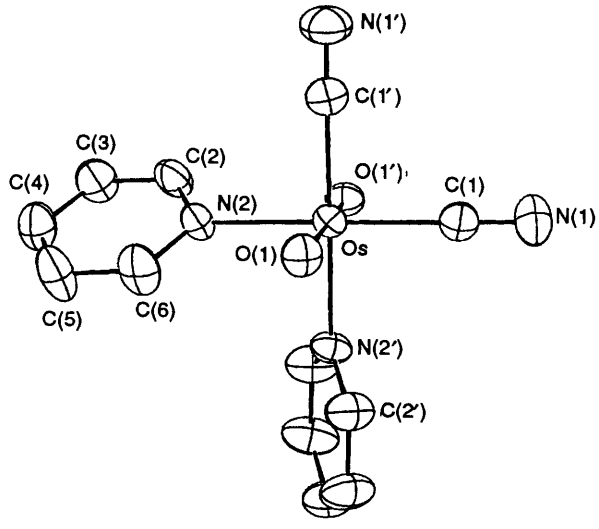

Fig. 4 Perspective view of $[Os^{VI}(py)_2(CN)_2(O)_2]$ **3**

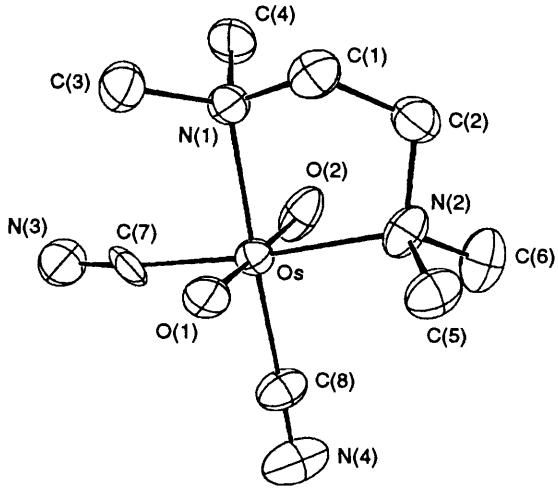

Fig. 5 Perspective view of $[Os^{VI}(tmen)(CN)_2(O)_2]$ **4**

respectively, whereas for **8**, the H(16)–O(1) and H(7)–O(2) distances are 1.90 and 1.93 Å respectively.

Extended-Hückel molecular-orbital calculations have been undertaken to study the effect on the electronic structure of *trans*-dioxoosmium(VI) of replacing CN^- by mesityl. The molecular orbital diagram calculated by the EHMO method is depicted in Fig. 8. The calculated highest occupied molecular orbital–lowest unoccupied molecular orbital (HOMO–LUMO) energy gaps are 1.08 eV for **4** and 0.74 eV for **8**. In complex **4**,

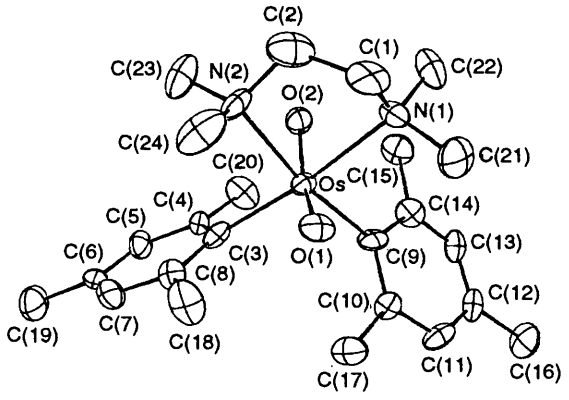

Fig. 6 Perspective view of $[Os^{VI}(mes)_2(tmen)(O)_2]$ **7**

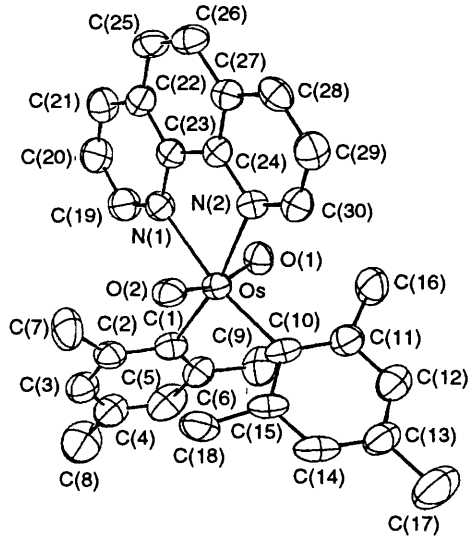

Fig. 7 Perspective view of $[Os^{VI}(mes)_2(phen)(O)_2]$ **8**

the HOMO has 79.7% d_{xy} orbital character and 17.1% due to the CN ligand. However, in **8**, the d_{xy} orbital character in the HOMO decreases to 53.7%, whereas 44.4% comes from the filled π orbitals of the mesityl ligands. In both complexes, the LUMO are predominated by the d_{π^*} of Os.

Electrochemistry.—The electrochemical data are listed in Table 5. The cyclic voltammograms of *trans*-$[Os(L–L)(CN)_2(O)_2]$ (L–L = 4,4′-Me_2bipy, 4,4′-Bu^t_2bipy or tmen) in acetonitrile display two reversible redox couples with $E°$ ranging from −0.88 to −1.02 and −1.67 to −2.09 V *vs.* Ag–$AgNO_3$ respectively. With reference to previous studies[13] on *trans*-$[Os^{VI}L^1O_2]^{2+}$ and related complexes, the former couple is assigned to Os^{VI}–Os^{V} and the latter to Os^{V}–Os^{IV}. Substitution of tmen by α-diimine ligands causes an anodic shift in the $E°$ values, and this is expected since a chelating tertiary amine should be a stronger base than an α-diimine.

Replacing CN^- by mesityl causes a cathodic shift in the $E°(Os^{VI}–Os^{V})$ values. Thus the Os^{VI}–Os^{V} couple of complex **7** occurs at −1.32 V, which is 0.30 V more cathodic than that of **4**. This is attributed to the stronger σ-donor strength of mesityl. In fact $[Os(mes)_2(L–L)(O)_2]$ shows an irreversible oxidation wave at +1.29 to +1.31 V owing to the oxidation of Os^{VI} to Os^{VII}.

Photophysical and Photochemical Properties.—At room temperature and upon excitation at 300–400 nm, most of the $[Os^{VI}(L–L)(X)_2(O)_2]$ (X = Cl^- or CN^-) complexes show weak photoluminescence with emission maxima at 651–730 nm. The emission data are listed in Table 6. In comparison with previous studies[15] on d^2 *trans*-dioxo metal complexes[2,14,15] the emitting state is due to the spin-orbit sublevels of the ^3E_g state; presumably the B_{1g} or B_{2g} sublevels in a C_{2v} symmetry. Complex **3** does not show any emission in solution at room temperature. Presumably, the non-rigidity of the two pyridine ligands would lead to a more efficient non-radiative decay of the excited state.

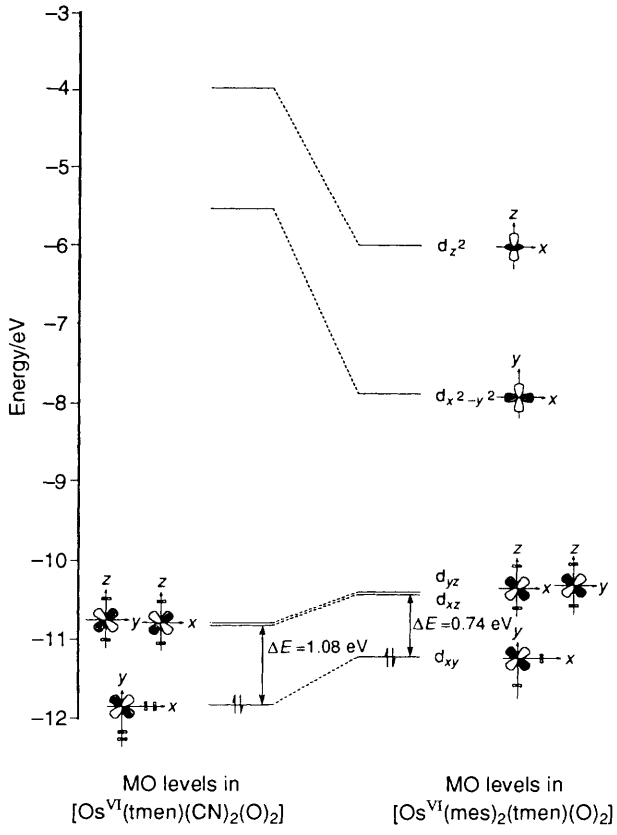

Fig. 8 An EHMO diagram of $[Os^{VI}(tmen)(CN)_2(O)_2]$ and $[Os^{VI}(mes)_2(tmen)(O)_2]$

On the other hand, complex **7** is not emissive in the solid state nor in solution. From the X-ray structural data, there is a close intramolecular contact between the Os=O unit and one of the C–H groups of the mesityl ligands. Whether or not this interaction may provide a non-radiative relaxation pathway for the excited state is not known.

Reactivity of trans-$[Os^{VI}(4,4'\text{-}Me_2bipy)(CN)_2(O)_2]$.—Complex **1** is a typical example of a neutral *trans*-dioxoosmium(VI) complex. It is interesting to compare its reactivity with that of *trans*-$[Os^{VI}L^1(O)_2]^{2+}$, the photochemical properties of which have been studied previously.[1,2] From the electrochemical data, complex **1** has a lower $E°(Os^{VI}–Os^{V})$ than that of *trans*-$[Os^{VI}L^1(O)_2]^{2+}$, yet the former complex is more reactive. For example, at room temperature *trans*-$[Os^{VI}L^1(O)_2]^{2+}$ does not react with PPh_3 in acetonitrile in the dark but **1** oxidizes PPh_3 to $O=PPh_3$ within minutes under the same conditions.

From the UV/VIS data, the Os=O bond of **1** in the excited state has a lower $\nu(OsO_2)$ (≈730 cm^{-1} estimated from the vibrational spacings in the UV/VIS absorption or excitation spectrum) than that in the ground state (846 cm^{-1}), indicating that the excited state is a good oxygen-atom donor. The excited state redox potential of **1** could be estimated by equation (4). The E_{0-0} value, estimated from the low-

$$E°(Os^{VI*}–Os^{V}) = E°(Os^{VI}–Os^{V}) + E_{0-0} \quad (4)$$

temperature solid-state emission spectrum, is 2.07 eV. Thus, $E°(Os^{VI*}–Os^{V})$ of **1** is estimated to be 1.77 V *vs.* NHE. The excited-state redox potential of the related $[Os^{VI}(L–L)$-

Table 5 Electrochemical data for $[Os^{VI}(L\text{–}L)(CN)_2(O)_2]$, $[Os^{VI}(L\text{–}L)Cl_2(O)_2]$ and $[Os^{VI}(mes)(L\text{–}L)(O)_2]$ and related complexes

Complex	$E°$/V (*vs.* Ag–$AgNO_3$) Reversible wave	Irreversible wave
1 $[Os^{VI}(4,4'\text{-}Me_2bipy)(CN)_2(O)_2]$[a]	−0.88, −1.67	—
2 $[Os^{VI}(4,4'\text{-}Bu^t_2bipy)(CN)_2(O)_2]$[a]	−0.89, −1.68	—
3 $[Os^{VI}(py)_2(CN)_2(O)_2]$[a]	—	−0.84, −1.21, −1.61
4 $[Os^{VI}(tmen)(CN)_2(O)_2]$[a]	−1.02, −2.09	—
5 $[Os^{VI}(bipy)Cl_2(O)_2]$[b]	—	−1.25
6 $[Os^{VI}(4,4'\text{-}Bu^t_2bipy)Cl_2(O)_2]$[b]	—	−1.25, −1.45
$[NBu_4]_2[Os^{VI}(CN)_2(O)_2(OH)_2]$[b]	—	−1.43
$[Os^{VI}L^1(O)_2]^{2+}$[b]	−0.66	—
$[As_2Ph_4]_2[Os^{VI}(CN)_4(O)_2]$[b]	−1.52	—
7 $[Os^{VI}(mes)_2(tmen)(O)_2]$[b]	−1.32	+1.31, −1.88
8 $[Os^{VI}(mes)_2(phen)(O)_2]$[b]	−1.24	+1.29

[a] In 0.1 mol dm^{-3} NBu_4PF_6–MeCN. [b] In 0.1 mol dm^{-3} NBu_4PF_6–CH_2Cl_2.

Table 6 Photophysical data for $[Os^{VI}(L\text{–}L)(CN)_2(O)_2]$ and $[Os^{VI}(L\text{–}L)Cl_2(O)_2]$ at 298 ± 2 K

Complex	Emission (λ_{max}/nm)	τ_o/μs	$10^4\ \Phi$	$E°(Os^{VI*}\text{–}Os^V)$/V (*vs.* NHE)
1 $[Os^{VI}(4,4'\text{-}Me_2bipy)(CN)_2(O)_2]$[a]	654	0.48	5.5	1.77
2 $[Os^{VI}(4,4'\text{-}Bu^t_2bipy)(CN)_2(O)_2]$[a]	653	0.49	6.3	1.72
3 $[Os^{VI}(py)_2(CN)_2(O)_2]$[a]	691 (solid state)	< 0.04	—	1.77
4 $[Os^{VI}(CN)_2(tmen)(O)_2]$[a]	651	0.41	5.7	1.63
5 $[Os^{VI}(bipy)Cl_2(O)_2]$[b]	729	0.49	1.2	1.18
6 $[Os^{VI}(4,4'\text{-}Bu^t_2bipy)Cl_2(O)_2]$[b]	730	0.50	1.1	1.17

[a] In degassed MeCN. [b] In degassed CH_2Cl_2.

Table 7 Photooxidation of substrate by $[Os^{VI}(4,4'\text{-}Me_2bipy)(CN)_2(O)_2]$ in degassed acetonitrile at 25 °C

Substrate	Products	Yield (%)
Triphenylphosphine	Triphenylphosphine oxide	—
Dimethyl sulfide	Dimethyl sulfoxide	100
Cyclohexene	Cyclohexen-2-one	36
	Cyclohexen-2-ol	36
	Cyclohexene oxide	28
Styrene	Styrene oxide	38
	Benzaldehyde	6
Norbornene	*exo*-2,3-epoxynorbornane	11
Cyclooctene	Cyclooctene oxide	29

$(CN)_2(O)_2]$ and $[Os^{VI}(L\text{–}L)Cl_2(O)_2]$ complexes are similarly determined and are listed in Table 6 from which it can be seen that the excited-state redox potential could be tuned from 1.17 to 1.77 V with ligand modification.

Despite complex **1** having a lower $E°(Os^{VI*}\text{–}Os^V)$ than of *trans*-$[Os^{VI}L^1(O)_2]^{2+}$, **1** functions as a better photooxidant. The results of the photooxidation of organic substrates by **1** are summarized in Table 7. Styrene is oxidized to styrene oxide in 38% yield. Under similar conditions, the photochemical reaction of *trans*-$[Os^{VI}L^1(O)_2]^{2+}$ with styrene gave styrene oxide in much lower yield and benzaldedyde was the major product. In the reaction with cyclohexene, the dominant products are cyclohexen-2-one and cyclohexen-2-ol (total over 72%) arising from allylic oxidation. Once again, this is in contrast to that of *trans*-$[Os^{VI}L^1(O)_2]^{2+}$, which gave cyclohexen-2-ol (25%) as the major product. Norbornene was photooxidized to *exo*-2,3-epoxynorbornane in 11% yield.

Conclusion

By ligand subsitution, a series of neutral *trans*-dioxoosmium(VI) complexes having tunable $E°(Os^{VI}\text{–}Os^V)$ and $E°(Os^{VI*}\text{–}Os^V)$ could readily be prepared. As with *trans*-$[Os^{VI}L^1(O)_2]^{2+}$ these complexes have long-lived and emissive excited states in solution at room temperature. While the neutral complexes have a lower excited state $E°(Os^{VI*}\text{–}Os^V)$ they could be more effective photooxidants for organic oxidation.

Acknowledgements

We acknowledge support from The University of Hong Kong and the Hong Kong Research Grants Council.

References

1 (*a*) C. M. Che, V. W. W. Yam and C. M. Che, *New J. Chem.*, 1989, **13**, 707; (*b*) V. W. W. Yam and C. M. Che, *Coord. Chem. Rev.*, 1990, **97**, 93.
2 V. W. W. Yam and C. M. Che, *J. Chem. Soc., Dalton Trans.*, 1990, 3741.
3 S. Schindler, E. W. Castner, jun., C. Creutz and N. Sutin, *Inorg. Chem.*, 1993, **32**, 4200.
4 G. M. Badger and W. H. F. Sasse, *J. Chem. Soc.*, 1956, 616.
5 B. S. McGilligan, J. Arnold, G. Wilkinson, B. H. Bates and M. B. Hursthouse, *J. Chem. Soc., Dalton Trans.*, 1990, 2465.
6 J. M. Malin, *Inorg. Synth.*, 1980, **20**, 61.
7 J. V. Houten and R. J. Watts, *J. Am. Chem. Soc.*, 1976, **98**, 4853.
8 SDP Structure Determination Package, Enraf-Nonius, Delft, 1985.
9 J. Howell, A. Rossi, D. Wallace, K. Haraki and R. Hoffmann, Quantum Chemistry Program Exchange (QCPE), 1977, no. 344.
10 K. A. Jorgensen and R. Hoffmann, *J. Am. Chem. Soc.*, 1986, **108**, 1867.
11 M. A. Thompson, *A Quantum Chemical Electronic Structure Program Version 1.1 User Manual*, 1992.
12 C. Sartori and W. Preetz, *Z. Anorg. Allg. Chem.*, 1989, 151.
13 C. M. Che, W. K. Cheng and V. W. W. Yam, *J. Chem. Soc., Dalton Trans.*, 1990, 3095.
14 V. M. Miskowski, H. B. Gray and M. D. Hopkins, personal communication.
15 J. R. Winkler and H. B. Gray, *Inorg. Chem.*, 1985, **24**, 346.

Received 4th April 1995; *Paper* 5/02159F